

# Structural Investigation of Stacked Multilayer Magnetic/Nonmagnetic Nanowires

\*Sobia Saher<sup>1)</sup>, M. Khaleeq-ur-Rehman<sup>2)</sup>, Saira Riaz<sup>3)</sup>  
and Shahzad Naseem<sup>4)</sup>

<sup>1)</sup> Centre for Advanced Studies in Physics, Govt. College University, Lahore, Pakistan  
<sup>2), 3), 4)</sup> Centre of Excellence in Solid State Physics, University of Punjab, Lahore,  
Pakistan

<sup>2)</sup> [khaleeq1953@gmail.com](mailto:khaleeq1953@gmail.com)

## ABSTRACT

Magnetic multilayer nanowires have been widely studied for many characteristics such as giant magnetoresistance (GMR) and tunneling magnetoresistance (TMR). Potentiostatic electrodeposition method is used to fabricate Ni, Ni/Cu/Ni, NiCo/Cu/NiCo and NiCoFe/Cu/NiCoFe single and multilayered nanowires. Above-mentioned stacks are repeated throughout the nanowires length of 6 $\mu$ m. Nanowires are grown in polycarbonate track etched membrane with nominal pore diameter ranging between 10 – 200nm. Diameter (30 nm) and length (6  $\mu$ m) of multilayered nanowires are kept fixed in order to study the effect of elemental and alloy ferromagnetic layers on giant magnetoresistance. Thickness of each ferromagnetic layer (i.e. Ni, NiCo, NiCoFe) is also kept fixed to around 6nm with 3nm non-magnetic spacer layer. XRD results reveal that nanowires exhibit crystalline structure under all conditions. Crystallographic texturing of the c-axis in the direction perpendicular to the NWs' long axis is observed in case of elemental Ni nanowires. Texturing of c-axis is observed to change when Ni/Cu/Ni multilayers are grown with same diameter and length. However, texturing of c-axis remains same for NiCo/Cu/NiCo and NiCoFe/Cu/NiCoFe stacks of multilayers. These variations are governed by the grain growth in Ni, Ni/Cu/Ni, NiCo/Cu/NiCo and NiCoFe/Cu/NiCoFe nanowires. Crystallite size of Ni, NiCo/Cu/NiCo and NiCoFe/Cu/NiCoFe is comparable to the pore diameter of polycarbonate template i.e. ~ 30nm thus showing c-axis in the direction perpendicular to the NWs' long axis.

## 1. INTRODUCTION

The use of nanostructured materials in electronic devices, optics, magnetic storage devices and sensors, tissue and cell engineering, other fields of biotechnology and medicine; with smallest features and dimensions below 100 nm, is the most important part of nanotechnology at present and in the near future. In the global market the number of nanoproducts and nanoengineered materials are rapidly increasing

because of a continuous revolution in fabrication methodology. Nanostructured materials such as nanoparticles, carbon nanotubes, quantum dots, quantum nanowires and nanocomposites allow completely new applications to be found because of their unique properties. Commercially available products now contain engineered nanomaterials including metals, ceramics, polymers, smart textiles, cosmetics, sunscreens, electronics, paints and varnishes. However, there is still a need to develop new methodologies and instrumentations to increase knowledge and information about their properties (Stergios Logothetidis 2012).

Nanowires are important building blocks of nanodevices and can serve as interconnects, active components in nanoscale electronic, optoelectronic, magnetic and photonic devices. In future, the nanowire based one-dimensional materials will be of prime importance in nanomaterials research. The achievement in the fabrication of nanowires using metals and their oxides and semiconductors is a scientific breakthrough. Synthesis of fine-tuned properties of nanowires has motivated researchers to envision radical and innovative fabrication methodologies for their implementation in novel applications. There are many challenges associated with the fabrication/synthesis of one dimensional nanostructures with controlled size, crystallinity, phase purity and chemical composition. The understanding and control of the nucleation and growth processes at the nanoscale is the key to fabricate precisely designed nanostructures (Sarkar 2007 and Shankar 2005).

Nanowires have one unconfined dimension and two quantum-confined dimensions, so their electrical conduction behavior is different from that of their bulk counterpart. In nanowires, tunneling and bulk conduction both take place in electronic conduction mechanism.

Both physical and chemical methods of deposition including Atomic Layer Deposition (ALD), Molecular Beam Epitaxy (MBE), Pulsed Laser Deposition (PLD), Magnetron Sputtering, Chemical Vapor deposition (CVD), Metal Organic Chemical Vapor deposition (MOCVD), spray pyrolysis, electrochemical deposition, Sol-gel etc. have been employed to grow nanostructures with controlled dimensions and good electrical, magnetic and optical properties. Among all deposition methods, electrodeposition has proved to be a simple, versatile, cost-effective and flexible technique to deposit nanostructures particularly template-assisted growth of nanowires. It is a unique technique in which a variety of materials can be processed including metals, semiconductors, ceramics and polymers. For synthesis of nanomaterials, controllable atomic scale deposition process is required and in comparison to other techniques electrochemical deposition provides atomic scale deposition. It can be used to synthesize nanostructures, nanowires and nanotubes. In electrodeposition process, various parameters such as electrolyte composition, solution pH, deposition time, deposition current and potential, temperature, etc. can be used to modify the physical and chemical properties of the deposits (Özkale 2015, Ramazani 2014, Bakonyi 2010, Gurrappa 2008, Liu 2003, Osaka 2000).

In the present work, both single and multilayer nanowires of different metals were fabricated by electrochemical deposition method from a single electrolyte in track – etched polycarbonate membranes, and their structural properties were studied.

## **2. Experimental Details**

For electrodeposition of nanowires, commercially available polycarbonate membrane (Nasirpouri 2007, Kazeminezhad 2007) with pore diameter of 30nm was used as template. One side of polycarbonate membrane was coated with 200nm Au film by evaporation to make a working contact electrode. The potentiostatic deposition was carried out in an electrochemical cell with three electrode configuration (Fig. 1). Saturated calomel electrode and a platinum sheet were used as reference electrode and counter electrode respectively. Pure Ni and multilayer Ni/Cu, NiCo/Cu and NiFeCo/Cu nanowires were prepared from a single electrolyte solution containing ions of Ni, Fe, Co and Cu ions. The pH of the electrolyte solutions was adjusted to a constant value of 2.8 and every time fresh solution was prepared to avoid contamination. The composition used for single and multilayer deposition and electrodeposition conditions are given in Table 1. The deposition parameters were optimized to overfill the pore of template for their structural analysis. The structural changes in all samples were investigated by Bruker D8 Advance X-Ray Diffractometer (XRD) using  $\text{CuK}\alpha$  (1.5406Å) radiations.

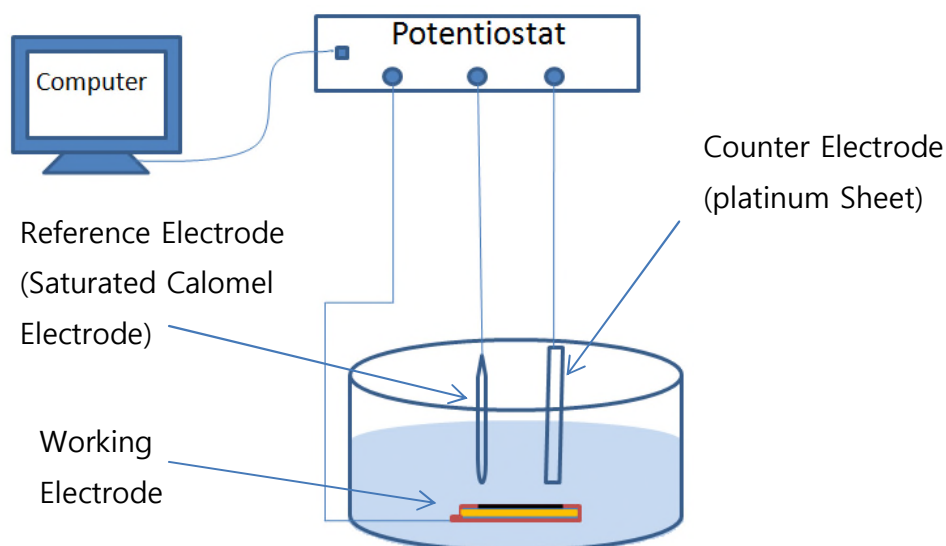


Fig. 1 Schematic diagram of electrodeposition setup

**Table1:** Composition of electrolyte solution and experimental conditions for nonowires

Experimental Condition	pH of electrolyte solution Deposition Temperature Cathode Potential for Ni, Co and Fe deposition Cathode Potential for Cu deposition	2.8 Room Temperature (25°C) - 1.2V -0.6V
Electrolyte Compositions	Pure Ni nanowires	0.2 M NiSO <sub>4</sub> .6H <sub>2</sub> O, 0.4 M H <sub>3</sub> BO <sub>3</sub>
	Ni/Cu multilayer nanowires	0.2 M NiSO <sub>4</sub> .6H <sub>2</sub> O, 0.0125 M CuSO <sub>4</sub> .5H <sub>2</sub> O, 0.4 M H <sub>3</sub> BO <sub>3</sub>
	NiCo/Cu multilayer nanowires	0.2 M NiSO <sub>4</sub> .6H <sub>2</sub> O, 0.05 M CoSO <sub>4</sub> .7H <sub>2</sub> O, 0.0125 M CuSO <sub>4</sub> .5H <sub>2</sub> O, 0.4M H <sub>3</sub> BO <sub>3</sub>
	NiFeCo/Cu multilayer nanowires	0.2 M NiSO <sub>4</sub> .6H <sub>2</sub> O, 0.05 M CoSO <sub>4</sub> .7H <sub>2</sub> O, 0.025 M FeSO <sub>4</sub> .7H <sub>2</sub> O, 0.0125 M CuSO <sub>4</sub> .5H <sub>2</sub> O, 0.4 M H <sub>3</sub> BO <sub>3</sub>

### 3. Results and Discussion

Fig. 2 shows XRD patterns of Ni and stacked multilayered Ni/Cu/Ni, NiCo/Cu/NiCo and NiCoFe/Cu/NiCoFe nanowires. Peaks at  $2\theta = 38.2^\circ$ ,  $44.5^\circ$ ,  $78.0^\circ$  and  $90.5^\circ$  in Fig. 2(a) correspond to Ni hexagonal closed pack (hcp) planes (010), (002), (011), (200), (220) and (202). These diffraction planes are in agreement with JCPDS card No. 45-1027. The rest of the peaks are from copper since it was deposited at the back of all templates. Peaks in stacked multilayered nanowire pattern of Ni/Cu/Ni (Fig. 2(b)) at  $44.2^\circ$ ,  $50.5^\circ$  and  $74.13^\circ$ ,  $78.0^\circ$  and  $90.5^\circ$  correspond to Ni and Cu planes. These diffractions peaks are in agreement with JCPDS Nos. 45-1027 and 4-0836, respectively. However, peaks at  $2\theta = 38.2^\circ$ ,  $46.5^\circ$  and  $81.8^\circ$  correspond to (010), (011) and (202) planes of hcp Ni. With incorporation of Cu in Ni peaks showed slight shifting in angles which is due to difference in ionic radii of copper (73pm) and nickel (69pm) (Figs. 3(a) and 3(b)). Peak at (200) plane matched with Ni as well as Cu. For NiCo/Cu/NiCo multilayers peaks at  $2\theta = 44.2^\circ$ ,  $50.5^\circ$  and  $90.5^\circ$  correspond to Co, Ni and Cu, respectively (Fig. 2(c)). For NiCoFe/Cu/NiCoFe multilayers  $2\theta = 46.5^\circ$  and  $81.8^\circ$  correspond to (110) and (211) planes of Fe. While peaks at  $2\theta = 39.0^\circ$ ,  $44.2^\circ$ ,  $50.5^\circ$  and  $74.4^\circ$  are matched with Ni, Co and Cu (Fig. 3(c)).

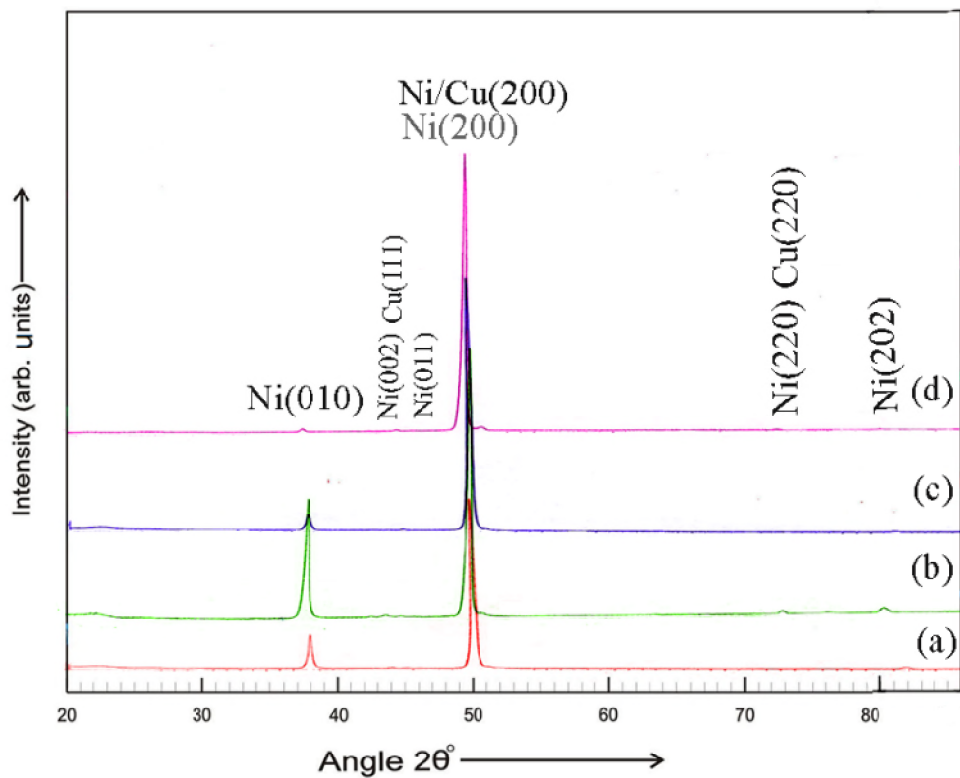
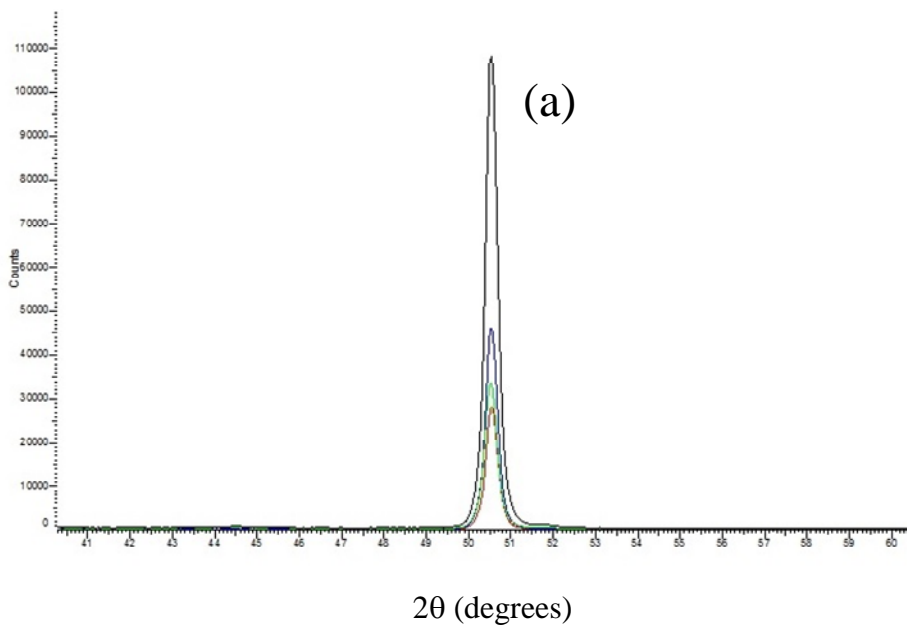


Fig. 2 Combined XRD patterns of multilayers (a) Ni (b) Ni/Cu/Ni (c) NiCo/Cu/NiCo and (d) NiCoFe/Cu/NiCoFe



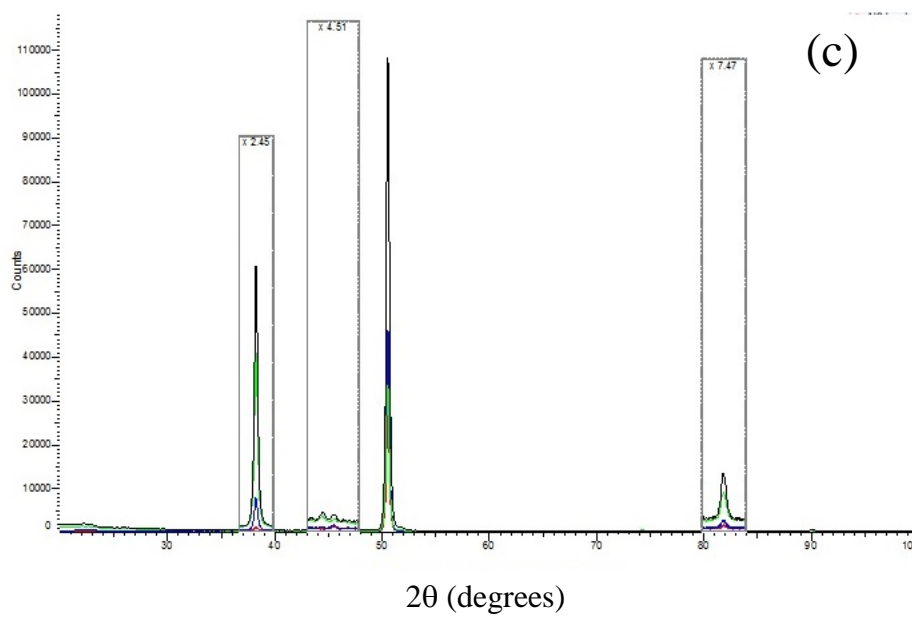
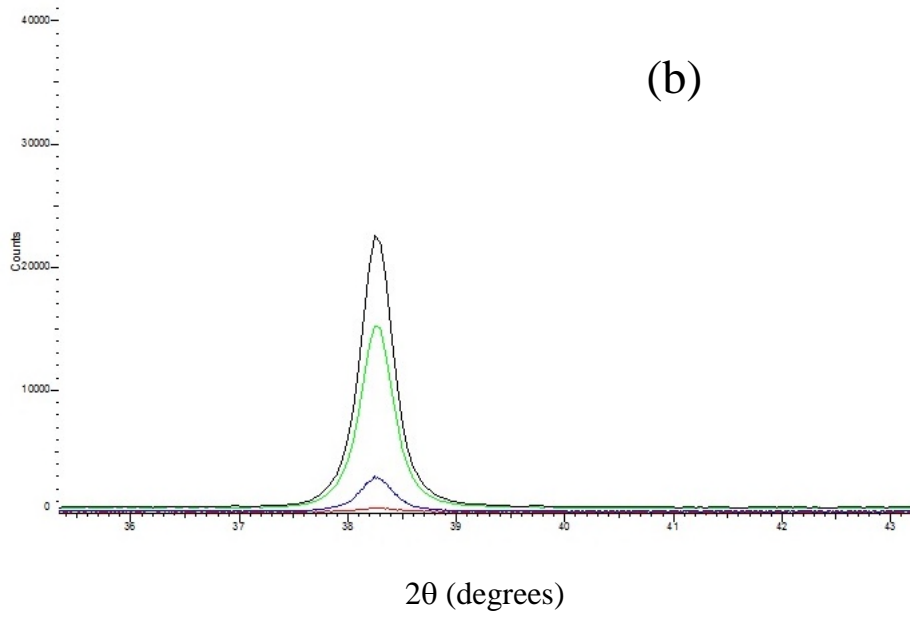


Fig. 3 XRD peaks at (a)  $2\theta=50.5^\circ$  showing shift in d-spacing, (b) same shift in d-spacing shown at around  $2\theta=38.0^\circ$  and (c) expanded views of smaller XRD peaks of elemental and stacked multilayers

Overall these results reveal that nanowires exhibit hexagonal close packed (hcp) crystal structure under all conditions. Crystallographic texturing of the c-axis in the direction perpendicular to the NWs' long axis was observed in case of elemental Ni nanowires. Texturing of c-axis was observed to change when Ni/Cu/Ni multilayers were grown with same diameter (30nm) and length (6 $\mu$ m). However, texturing of c-axis remained same for NiCo/Cu/NiCo and NiCoFe/Cu/NiCoFe stacks of multilayers as shown in Fig. 3. Such texturing might have been observed because of the lattice energy that is responsible to control lattice mismatch when thickness of individual layer is quite thin i.e. ~ 3nm.

Crystallite size and dislocation density of Ni nanowires and stacked multilayered nanowires was estimated using Eqs. 1 and 2 (Cullity 1956).

$$D = 0.9\lambda / B \cos \theta \quad (1)$$

$$\delta = 1 / D^2 \quad (2)$$

Where D is crystallite size,  $\lambda$  is wavelength of X-rays used (1.5406 $\text{\AA}$ ), B is full width at half maximum,  $\theta$  is diffraction angle and  $\delta$  stands for dislocation density.

Crystallite size of the of nickel nanowires was calculated to be 29.8nm. Decrease in crystallite size of Ni/Cu/Ni was observed. This decrease in crystallite size might have been observed because of the re-structuring in the crystal structure. This is evident from the values of crystallinity shown in Fig. 4. Such re-structuring is accompanied by change in the preferred orientation of nanowires which may lead to change in easy axis of nanowires. Furthermore, crystallite size was observed to increase when ferromagnetic elemental layer, i.e. Ni, was replaced by alloy ferromagnetic layer, i.e. NiCo. This increase might have been observed because of the availability of more ferromagnetic sites for nucleation and then coalescence. Similar increasing trend in crystallite size was observed when binary ferromagnetic alloy was replaced by ternary ferromagnetic alloy. Crystallite size of Ni, NiCo/Cu/NiCo and NiCoFe/Cu/NiCoFe is equal to the pore diameter of polycarbonate template i.e. ~ 30nm thus showing c-axis in the direction perpendicular to the NWs' long axis.

Variation in crystallite size and dislocation lines/m<sup>2</sup> (dislocation density) is shown in Figs. 4 and 5. These variations are governed by the grain growth in Ni, Ni/Cu/Ni, NiCo/Cu/NiCo and NiCoFe/Cu/NiCoFe nanowires as discussed earlier.

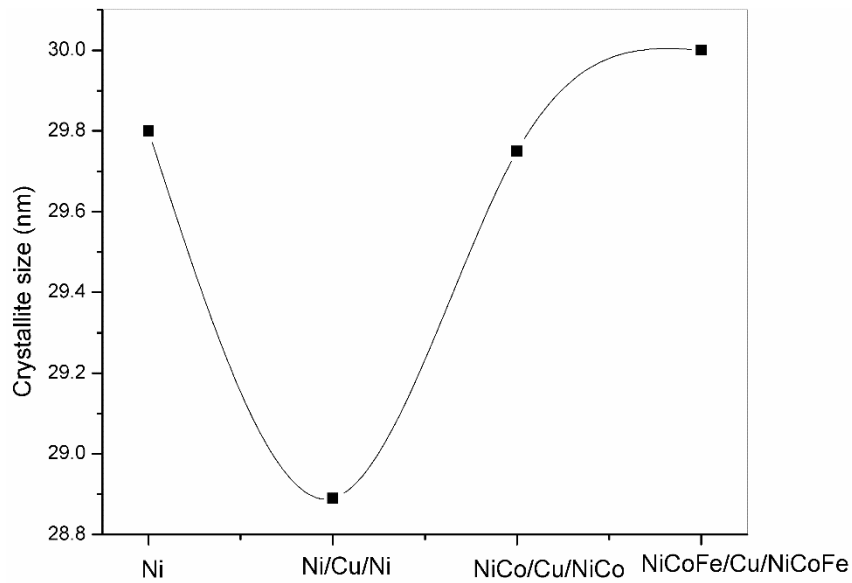


Fig. 4 Variation in crystallite size of multilayers

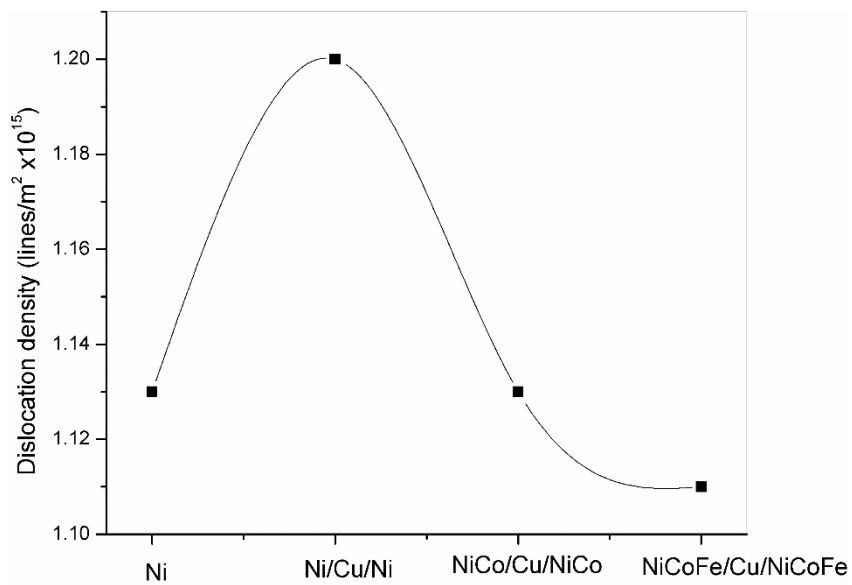


Fig. 5 Variation in dislocation density of multilayers

Crystallinity of multilayers was calculated as a sum of the crystalline fractions present in the depositions, with the balance being amorphous. In this study sharp diffraction lines were observed in the XRD patterns of the multilayers. The sharp diffraction lines with low/minimum background noise showed that these multilayers have good crystallinity. Fig. 6 shows variation in crystallinity of Ni and stacked multilayered nanowires. It is interesting to note that crystallinity and crystallite size show similar trends. This leads to validations of earlier statement of re-structuring taking place in the presence of more depositions and / or increasing the number of metals in the ferromagnetic alloy. Such re-structuring has previously been reported (Riaz and



Naseem, 2007) for metallic elemental layer deposition. Effect of this re-structuring on magnetic properties of these stacked nanowires are to be reported elsewhere (Sobia et al. 2016).

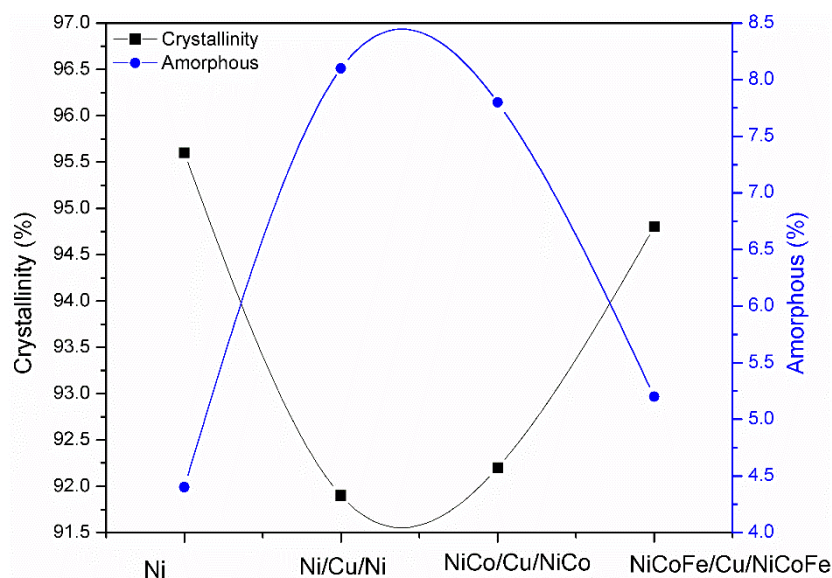


Fig. 6 Variation in crystallinity and amorphous behavior of multilayers

### 3. CONCLUSIONS

Stack of multilayered magnetic and non-magnetic nanowires were grown in polycarbonate track etched membrane. Thickness of each ferromagnetic layer (i.e. Ni, NiCo, NiCoFe) was kept fixed to ~6nm with 3nm non-magnetic spacer layer. XRD results revealed that nanowires exhibited crystalline structure under all conditions. Crystallographic texturing of the c-axis in the direction perpendicular to the NWs' long axis was observed in case of elemental Ni and NiCo/Cu/NiCo and NiCoFe/Cu/NiCoFe nanowires. Crystallite size of Ni, NiCo/Cu/NiCo and NiCoFe/Cu/NiCoFe was comparable to the pore diameter of polycarbonate template i.e. ~ 30nm thus showing c-axis in the direction perpendicular to the NWs' long axis.

## REFERENCES

- Bakonyi, I. and Peter, L. (2010), "Electrodeposited multilayer films with giant magnetoresistance (GMR): Progress and problems," *Prog. Mater. Sci.*, **55**, 107–245.
- Cullity, B.D. (1956), *Elements of X-Ray Diffraction*, Anderson and Wiley Publishers, USA.
- Gurrappa, I. and Binder, L. (2008), "Electrodeposition of nanostructured coatings and their characterization - a review," *Sci. Technol. Adv. Mater.*, **9**, 043001-043012.
- Kazeminezhad, I., Barnes, A.C., Holbrey, J.D., Seddon, K.R. and Schwarzacher, W. (2007), "Templated electrodeposition of silver nanowires in a nanoporous polycarbonate membrane from a nonaqueous ionic liquid electrolyte," *Appl. Phys. A*, **86**, 373–375.
- Liu, X., Zangari, G. and Shamsuzzoha, M. (2003), "Structural and Magnetic Characterization of Electrodeposited, High Moment FeCoNi Films," *J. Electrochem. Soc.*, **150**, C159-C168.
- Logothetidis, S. (2012), *Nanostructured Materials and Their Applications*, Springer-Verlag Berlin, Heidelberg.
- Nasirpouri, F., Southerna, P., Ghorbanib, M., Zadb, A.I. and Chwarzacher, W. (2007), "GMR in multilayered nanowires electrodeposited in track-etched polyester and polycarbonate membranes," *J. Mag. Mag. Mater.*, **308**, 35–39.
- Osaka, T. (2000), "Electrodeposition of highly functional thin films for magnetic recording devices of the next century," *Electrochim. Acta*, **45**, 3311–3321.
- Ozkale, B., Shamsudhin, N., Chatzipirpiridis, G., Hoop, M., Gramm, F., Chen, X., Marti, X., Sort, J., Pellicer, E. and Pane, S. (2015), "Multisegmented FeCo/Cu Nanowires: Electrosynthesis, Characterization, and Magnetic Control of Biomolecule Desorption," *Appl. Mater. Interf.*, **7**, 7389–7396.
- Ramazani, A., Ghaffari, M., Kashi, M.A., Kheiry, F. and Eghbal, F. (2014), "A new approach to fabricating magnetic multilayer nanowires by modifying the ac pulse electrodeposition in a single bath," *J. Phys. D: Appl. Phys.*, **47**, 355003-355014.
- Riaz, S. and Naseem, S. (2007), "Effect of Reaction Temperature & Reaction Time on the Structural Properties of CIGS Thin Films Deposited by Sequential Elemental Layer Technique," *J. Mater. Sci. Technol.*, **23**, 499-503.
- Saher, S., Khaleeq-ur-Rehman, M. Riaz, S. and Naseem, S. (2016) "Investigations of dependence of magnetic properties on the structural changes in stacked multilayered magnetic / non-magnetic nanotubes", *Nanomaterials*, to be submitted.
- Sarkar, J., Khan, G.G. and Basumallick, A. (2007), "Nanowires: properties, applications and synthesis via porous anodic aluminium oxide template," *Bull. Mater. Sci.*, **30**, 271–290.
- Shankar, K.S. and Raychaudhuri, A.K. (2005), "Fabrication of nanowires of multicomponent oxides: Review of recent advances," *Mater. Sci. Eng. C*, **25**, 738 – 751.